express
polymer letters

Research article

Bio-renewable furan-based poly(ester amide)s: Synthesis, structure, spectroscopic and mechanical properties of poly(hexylene 2,5-furandicarboxylate)-*co*-poly(propylene furanamide)s (PHF-*co*-PPAF)

Agata Zubkiewicz[1]*, Izabela Irska*[2], *Konrad Walkowiak*[2], *Jerzy Dryzek*[3], *Sandra Paszkiewicz*[2]

[1]Faculty of Mechanical Engineering and Mechatronics, Department of Technical Physics, West Pomeranian University of Technology, Piastów Av. 48, 70311 Szczecin, Poland
[2]Faculty of Mechanical Engineering and Mechatronics, Department of Materials Technologies, West Pomeranian University of Technology, Piastów Av. 19, 70310 Szczecin, Poland
[3]Institute of Nuclear Physics, Polish Academy of Sciences, PL 31342, Kraków, Poland

Abstract. In this work, new furan-based poly(ester amide)s of various compositions were synthesised by the melt polycondensation method. The chemical structure and composition were determined by nuclear magnetic resonance spectroscopy (^{1}H NMR) and Fourier transform infrared (FTIR) analyses. The optical properties were studied by UV-Vis spectroscopy. The thermal properties were investigated by means of differential scanning calorimetry (DSC). The thermo-oxidative stability of PEAs was also tested. Additionally, the free volume by positron annihilation lifetime spectroscopy (PALS) technique and mechanical properties were examined. It was found that the incorporation of poly(propylene furanamide) (PPAF) units significantly affects the thermal and mechanical properties of co-polymers based on poly(hexylene 2,5-furandicarboxylate) (PHF). Depending on the composition, both semi-crystalline and amorphous co-polymers were obtained. Moreover, the values of the free volume radius (R) and the free volume fractions (f_v) were strongly affected by the mole fraction of PPAF units.

1. Introduction

Polymeric materials are widely used in many areas of life, and their popularity is influenced by low production cost and desired properties. Unfortunately, most polymers are based on petrochemicals and are nonbiodegradable, which has a negative impact on the environment. Greenhouse gas emissions and the depletion of natural resources were among the main reasons for the search for new polymers obtained from renewable raw materials. Many years of research have shown that 2,5-furandicarboxylic acid (FDCA) and its derivatives are one of the most promising monomers for the synthesis of bio-based polyesters, polyurethanes, or polyamides. Replacing terephthalic acid with 2,5-furanedicarboxylic acid allows obtaining materials with often improved properties than their petroleum-based counterparts. In particular, the literature has extensively described the improvement of barrier properties which are extremely important in the packaging industry [1–4]. In recent years, FDCA-based polyesters such as poly(ethylene 2,5-furanedicarboxylate) (PEF) [5–8], poly(propylene 2,5-furanedicarboxylate) (PPF) [9–13] and poly(butylene 2,5-furanedicarboxylate) (PBF)

---

*Corresponding author, e-mail: agata.zubkiewicz@zut.edu.pl

[14–18] have been studied in detail. Also, poly(hexamethylene 2,5-furanedicarboxylate) (PHF) aroused the interest of researchers [19–21], however, to our knowledge, poly(ester amide)s based on PHF have not been studied so far.

Poly(ester amide)s (PEAs) are interesting materials because of the combination of the advantages of polyamides, such as excellent mechanical and thermal properties and polyesters, which are often biodegradable. Over the past decades, many PEAs have been synthesised and investigated. Hydrolysable ester groups contribute to the degradable nature of these materials. As an example, Montané *et al.* [22] reported the preparation and characterisation of PEAs derived from 1,4-butanediol, sebacic acid, and L-alanine or glycine. These polymers showed susceptibility to hydrolytic and enzymatic degradability. Depending on the material, degradation conditions, and the enzyme used, the sample could be completely degraded after just 4 days. Other degradable PEAs have been investigated by Wang *et al.* [23] and obtained from 1,4-butanediol, 1,10-decanediamine, 1,10-sebacic acid, and itaconic acid. An in vitro degradation study showed a weight loss of over 30% after 50 days. The study of PEAs has repeatedly proven their susceptibility to degradation. The weight loss depended not only on the time and conditions of incubation but also on the degree of crystallinity and composition of co-polymers [24]. The amide groups between which strong hydrogen bonds are formed, in turn, contribute to the increased mechanical strength and thermal resistance of PEAs. The improvement of the mechanical properties of PEAs in relation to the corresponding polymer or co-polymer without amide groups was reported, among others, by Yang *et al.* [25] and Lips *et al.* [26].

The combination of these advantages of polyamides and polyesters makes PEAs seem to be ideal materials for many applications, especially in medicine, such as drug delivery systems, scaffolds in tissue engineering, hydrogels, or smart materials. Thanks to the possibility of obtaining various types of compositions, differing in the ratio of amide groups to ester groups, it is possible to obtain a wide range of materials with various properties and a wide range of applications. However, obtaining polyamides and poly(ester amide)s from 2,5-furandicarboxylic acid or its derivatives, turned out to be a great challenge. The decarboxylation of FDCA and the production of by-products often resulted in the formation of low

molecular weight materials [27, 28]. As is reported in the literature, attempts have been made to synthesise polyamides and PEAs based on FDCA by various methods such as direct polycondensation [29–31], interfacial polymerisation [29, 32–34], solution polymerisation [35–37], solid-state polymerisation [27, 38] or enzymatic polymerisation [39–41], but usually low molecular weights or amorphous materials were obtained. The fact that most of the FDCA-based polyamides and PEAs described in the literature were incapable of crystallisation is often influenced by the low molecular weight, which prevents the tight packing of molecules and the formation of hydrogen bonds between the amide protons and the oxygen atom in the furan ring, preventing the formation of intermolecular hydrogen bonds [42, 43]. Obtaining semi-crystalline poly(ester amide)s based on FDCA is possible when there is an appropriate spacer between the amide group and the furan ring. This strategy was used, for example by Papadopoulos, who, however, achieved relatively low intrinsic viscosities, not exceeding 0.45 dl/g [44]. The problem of low molecular weight also appeared, among others, in the work of Maniar *et al.* [41], who obtained semi-crystalline poly(amide ester)s by enzymatic polymerisation. It is also worth noting that there is very little literature data on the mechanical properties of FDCA-based poly(ester amide)s.

In our earlier paper, we reported the synthesis, structure, and thermal and mechanical properties of new poly(trimethylene 2,5-furandicarboxylate)-*co*-poly(propylene furanamide)s (PTF-*co*-PPAF) [45]. The obtained co-polymers, due to the introduction of amide units, were characterised, among others, by increased thermal and thermo-oxidative stability, and increased Young's modulus. However, all the synthesised materials were amorphous. As is known, semi-crystalline polymers generally show better thermal and chemical resistance and are characterised by greater wear resistance. In addition to amorphous ones, semi-crystalline biobased PEAs are also sought for extending the potential use of poly(ester amide)s. Biobased PEAs could be suitable for a wide variety of applications in the packaging industry, in the manufacture of fibres, and even in biomedicine. However, good mechanical and thermal properties are crucial in these applications.

In this study, which was a continuation of our previous work, poly(trimethylene 2,5-furandicarboxylate) was replaced with easily crystallising poly(hexamethylene

2,5-furandicarboxylate), resulting in new poly(hexamethylene 2,5-furandicarboxylate)-*co*-poly(propylene furanamide)s (PHF-*co*-PPAF). The synthesis and the influence of the PPAF units' content on the thermal, and mechanical properties have been studied. To the best of our knowledge, this is the first report on the synthesis and properties of PHF-*co*-PPAF co-polymers.

2. Experimental section
2.1. Synthesis of poly(ester amide)s
The series of poly(hexylene 2,5-furandicarboxylate)-*co*-poly(propylene furanamide) (PHF-*co*-PPAF) copolymers were obtained using two-stage melt polycondensation process of dimethyl furan 2,5-dicarboxylate (DMFDC, 99%, Henan Coreychem Co., Ltd., Zhengzhou, China), 1,6-hexylene glycol (HDO, Rennovia Inc., Santa Clara, CA, USA), 1,3-propylene glycol (bio-PDO, DuPont Tate & Lyle BioProducts, Loudon, USA) and 1,3-diaminopropane (DAP, >99%, Sigma Aldrich). Syntheses were carried out in a 1 dm³ steel reactor (Autoclave Engineers, Pennsylvania, USA) equipped with a stirrer, gas inlet, condenser, and vacuum pump. First, in a typical procedure, the transesterification of DMFDC with HDO, PDO, and DAP in the presence of titanium (IV) butoxide (Fluka) as a catalyst, and Irganox 1010 (Ciba-Geigy, Switzerland) as an antioxidant, took place. The reaction proceeded at 165–190 °C until the appropriate amount of by-product (methanol, ~90% of theoretical value) was distilled off. In the second step, the second portion of the catalyst was added, the temperature was gradually increased up to 240 °C, and the pressure was reduced below 20 Pa. The reaction was stopped when the melt reached a specified viscosity value, and the torque was at the same specified value for all materials. In the end, the final product was extruded from the reactor under nitrogen pressure, cooled in a water bath, and then granulated.

2.2. Sample preparation
The dumbbell type specimens (type A3) for tensile tests and FTIR measurements were prepared by injection moulding (Dr BOY GmbH and Co., Germany) with the following processing conditions: injection temperature: 180 °C, mould temperature: 30 °C, injection pressure: 40 MPa, holding down pressure: 25 MPa, time of holding down pressure: 5 s and cooling time: 30 s.

Thin polymer films for UV-VIS measurements with a thickness of about 200 μm were prepared by compression moulding (Collin P 200E) at a temperature of about 30 °C higher than their melting point. Compression of the samples was carried out in three stages: pressing for 60 s under a pressure of 5 bar, pressing for 90 s under a pressure of 50 bar, and cooling under a pressure of 50 bar.

2.3. Characterisation methods
The intrinsic viscosity (*IV*) measurements were carried out in a Ubbelohde Ic capillary viscosimeter ($K = 0.03294$) at 30 °C. Polymer solutions were prepared with concentrations of 0.5 g/dl in a phenol/1,1,2,2-tetrachloroethane (60/40 wt%, Sigma Aldrich) mixture.

NMR spectroscopy of the co-polymers was performed on a Bruker Spectrometer operated at 400 MHz, using chloroform-d (CDCL₃) with a few drops of trifluoroacetic acid (CF₃COOH) as solvents. ¹H NMR spectra of solutions with a concentration of 10 mg/ml were recorded at room temperature and calibrated to tetramethylsilane (TMS) as an external reference. Before the experiment, all samples were subjected to Soxhlet extraction with methanol for 48 h to remove impurities and possible low-molecular weight products. The real mole fractions of PPAF units were calculated from the determined integral intensities of the characteristic peaks, according to Equation (1):

$$W_{PPAF} = \frac{2I_f}{2I_f + I_b} \cdot 100\% \qquad (1)$$

where I_b and I_f are the integral signal intensities, corresponding to –OCH₂ (4H, PHF units) protons and -CH₂ (2H, PPAF units) protons, respectively.

The number average (M_n) and weight average (M_w) molecular weights were determined by Size Exculsion Chromatography (SEC) using Waters system composed of Waters 1515 Isocratic HPLC pump, a Waters 2414 refractive index detector (35 °C), a Waters 2707 autosampler, and a PSS PFG guard column followed by two PFG-linear-XL (7 μm, 8×300 mm) columns in series. 1,1,1,3,3,3-hexafluoroisopropanol (HFIP) with potassium trifluoroacetate was used as the eluent, The flow rate was 0.8 ml/min. The SEC was calibrated using poly(methyl methacrylate) standards.

The FTIR measurements were performed by means of a Nicolet 380 ATR-FTIR spectrometer (Thermo

Scientific, USA). Each sample was scanned 16 times in the range of 4000–400 cm⁻¹.

UV-Vis spectra were carried out on a UV-Vis spectrometer (UV-1800, Shimadzu, Kioto, Japan). Films with a thickness of 200±10 µm were scanned in the range of 350–800 nm with a 1 nm interval.

Differential scanning calorimetry (DSC) was performed with a DSC 204 F1 Phoenix (Netzsch, Selb, Germany). The samples of about 10 mg were encapsulated in aluminium pans and heated up/cooled down under nitrogen flow with a heating/cooling rate of 10, 5, 3, and 1 °C/min. The degree of crystallinity (x_c) was calculated by Equation (2):

$$X_c = \frac{\Delta H_m - \Delta H_{cc}}{\Delta H_m^0} \cdot 100\% \qquad (2)$$

where ΔH_m and ΔH_{cc} are the melt and cold crystallisation enthalpies, respectively, and ΔH_m^0 is the heat of fusion of 100% crystalline PHF (143 J/g [21]). Thermo-oxidative stability of PHF-*co*-PPAF co-polymers was evaluated using thermogravimetric analysis (TGA 92-16.18 SETARAM Instrumentation, Caluire-et-Cuire, France). Samples were heated under oxidising atmosphere (dry, synthetic air – $N_2:O_2$ = 80:20 vol%) from 20 to 700 °C, at a heating rate of 10 °C/min. Measurements were conducted in accordance with the PN-EN ISO 11358:2004 standard.

Positron annihilation lifetime spectroscopy (PALS) measurements were conducted on TechnoAp digital positron lifetime spectrometer with a timing resolution of 190 ps. The positron source was ²²NaCL between two thin Kapton foils (7 µm). Two Hamamatsu H3378-50 photomultipliers coupled with a single crystal of BaF2 scintillators from KristalKort were used to detect annihilation and 1.27 MeV gamma photons. Over a million counts were collected in each

spectrum. All obtained spectra were deconvoluted using the LT-Polymer code.

Tensile tests were conducted at room temperature on a universal testing machine (Autograph AG-X plus, Shimadzu), equipped with an optical extensometer, 1 kN Shimadzu load cell, and the TRAPEZIUM X computer software in a tensile configuration according to EN ISO 527. Dumbbell shape samples were stretched at a rate of 1 mm/min up to 1% of strain to calculate the tensile modulus and then at a rate of 5 mm/min until breakage. Five measurements were performed for each sample, and the results were averaged.

3. Results and discussion
3.1. Structure and composition
As shown in Table 1, the intrinsic viscosities of PHC-*co*-PPAF samples were within the range of 0.829 to 1.067 dl/g. It is very worthy to note that for the two extreme compositions of poly(ester amide)s, the intrinsic viscosities were the highest and were close to 1. In general, the higher the intrinsic viscosity, the higher the molecular mass of a polymer. The flexibility of the chains can also influence the *IV* value. In the case of neat PHF polyester, the obtained intrinsic viscosity was greater than in our previous study [19].

The molecular weights determined by SEC and summarised in Table 1 expose that all obtained poly(ester amide)s have a number average molecular weight (M_n) greater than 27 000 g/mol. It is worth noting that molecular mass values showed the same trend as the *IV* values. As in the case of the *IV*, the extreme compositions of poly(ester amide)s are characterised by the highest values of M_n. Moreover, the ratio of M_w to M_n was used to calculate the molecular-weight

Table 1. Composition and intrinsic viscosities of PHF-*co*-PPAF poly(ester amide)s.

Material	W_{PHF} [mol%]	W_{PPAF} [mol%]	W_{PPAF}^{NMR} [mol%]	*IV* [dl/g]	M_n [g/mol]	M_w [g/mol]	*D* [–]
PHF	100	0	0	0.825	29928	80106	2.67
PHF-*co*-PPAF 1/0.06	94	6	7.47	1.067	38869	111165	2.86
PHF-*co*-PPAF 1/0.16	84	16	15.25	0.876	29600	82584	2.79
PHF-*co*-PPAF 1/0.25	75	25	24.24	0.829	27935	81849	2.93
PHF-*co*-PPAF 1/0.50	50	50	45.05	1.022	31498	100163	3.18

W_{PHF} – mole fractions of PHF units;
W_{PPAF} – mole fractions of PPAF units;
W_{PPAF}^{NMR} – mole fraction of PPAF units determined by ¹H NMR;
IV – intrinsic viscosity;
M_n – number average molecular weight;
M_w – weight average molecular weight;
D – molecular weight dispersity.

dispersity (*D*). The *D* of the obtained materials increases with the incorporation of PPAF units and ranges from 2.67 for neat PHF to 3.18 for PHF-*co*-PPAF 1/0.50 co-polymer. Typically, polymers obtained by the two-step melt polycondensation method have *D* values close to 2, since when two different monomers are involved, a stoichiometric imbalance occurs, and the classical Flory's most probable distribution is no longer valid. In the case of stoichiometric imbalance, one will never be able to incorporate all monomer units into a single chain like in chain transfer or radical polymerisation (as it will theoretically occur at stoichiometric balance), and therefore, smaller chains will always be present due inevitable side reactions during the synthesis, favoured by the high reaction temperature. The larger the imbalance, the higher will be the difference in size between the chains. However, the obtained *D* values are not as high as in the case of another reported furan-based poly (ester amide)s synthesised by a similar method [43], and the high molecular weights indicate that relatively good quality materials were obtained. The ^{1}H NMR spectra of PHF and PHF-*co*-PPAF poly(ester amide)s are illustrated in Figure 1. The peaks' assignment of the PHF has been described in detail elsewhere [19, 21, 46]. The resonances at around 4.33, 1.79, and 1.48 ppm correspond to the protons of the methylene groups in the hexylene glycol subunit. The characteristic peak attributed to the protons of the furan ring is observed at 7.19 ppm. Moreover, as it can be seen, in the 7–7.5 ppm range a peak attributed to the solvent is visible and small signals likely due to the presence of low molecular weight products can be observed for PTF-*co*-PPAF 1/0.16 and PTF-*co*-PPAF 1/0.25 co-polymers. Furthermore, for poly(ester amide)s, new signals associated with PPAF units appeared. As in our previous publication, the signal from the protons of the methylene groups bonded to the nitrogen atom appeared at 3.63 [45]. The weak signal at 2.1 ppm is attributed to the middle methylene group belonging to the 1,3-propanediol. Besides, a new peak occurring at 3.98 ppm can be ascribed to amide protons. The molar ratios of PPAF in PHF-*co*-PPAF poly(ester amide)s were calculated by integrating the peaks' area in the ^{1}H NMR spectrum. The calculated poly(ester amide)s compositions, along with the theoretical values are presented in Table 1. Generally, the calculated molar fractions of PPAF for all synthesised materials are close to the theoretical values. Only in the case of
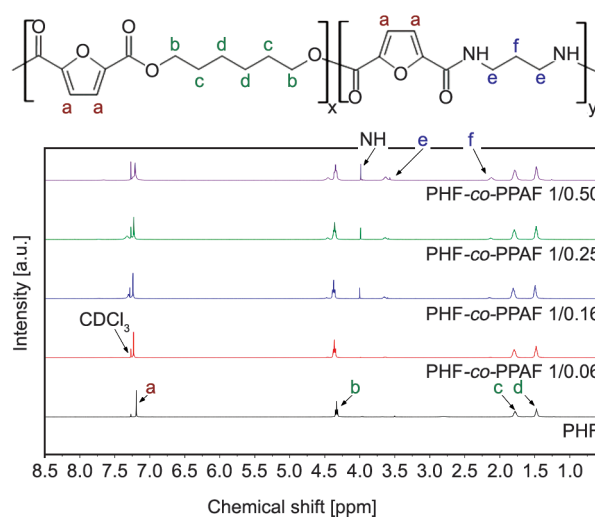

Figure 1. ^{1}H NMR spectra of PHF and PHF-*co*-PPAF poly(ester amide)s.

the PEA with the highest content of PPAF units, the difference was over 4%.

The chemical structure of PHF-*co*-PPAF poly(ester amide)s was further assessed by FTIR spectroscopy (Figure 2). Pure PHF shows two bands at 1217–1267 cm^{-1} corresponding to the =C–O–C= stretching. A more intense band due to the antisymmetric stretching appears at 1267 cm^{-1}, and the less intense corresponding to the ring vibration was observed at 1217 cm^{-1}. Moreover, high-intensity peaks at 1575 and 3117 cm^{-1}, related to the C=C stretching bonds and C-H stretching bonds, were observed. The stretching vibration peaks of C=O appear at around 1716 cm^{-1}. The absorption bands of methylene groups are visible at 2941 cm^{-1}. There are also three signals due to the furan ring bending at 767, 816, and 966 cm^{-1}, and a breathing signal observed at 1018 cm^{-1}. These spectra are in agreement with those in the literature [19, 47].

The spectra of poly(ester amide)s are very similar to PHF, except for characteristic signals derived from the amine groups. One can observe the presence of absorption bands at around 3374 cm^{-1} attributed to the stretching vibrations of hydrogen-bonded N–H groups (Figure 2b). Nevertheless, these signals are extremely weak, indicating that the formation of intramolecular hydrogen bonds is limited. Moreover, no bands corresponding to free N–H groups were observed. As noted in the literature, for polyamides and PEAs, typically between 3300 and 3450 cm^{-1}, two intense peaks correspond to the stretching vibration of the N–H groups [32, 43, 48, 49]. In addition, peaks attributed to the amide I and amide II bending
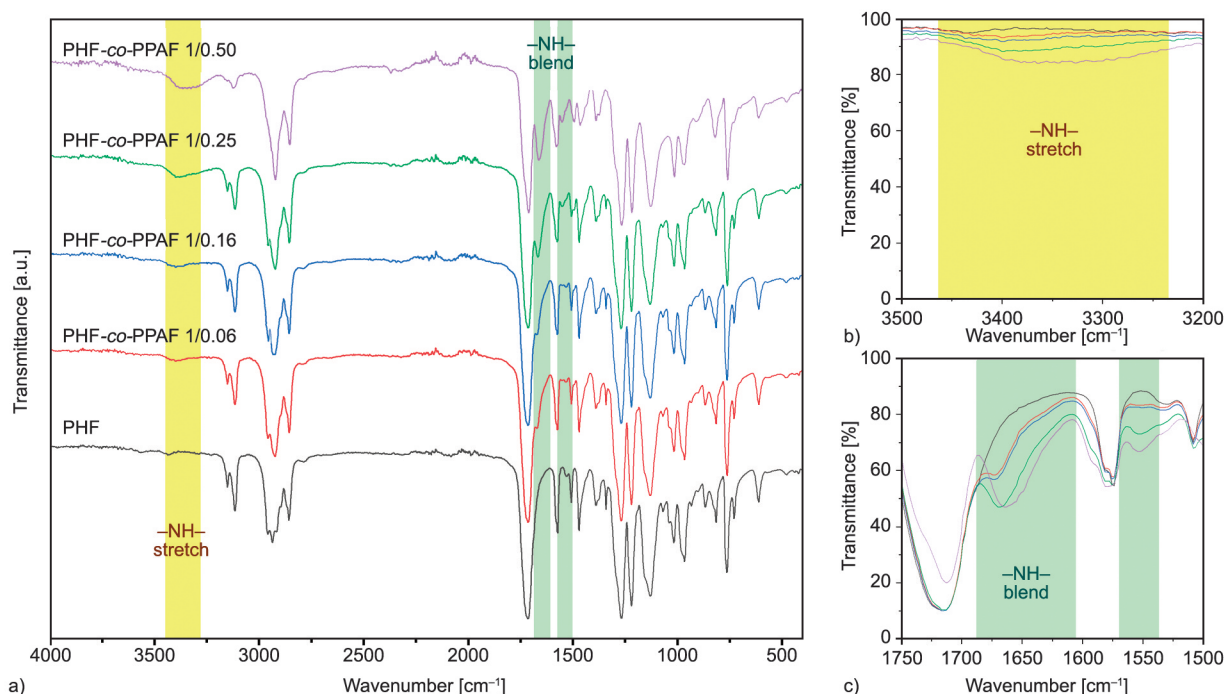
Figure 2. FTIR spectra of PHF and PHF-*co*-PPAF poly(ester amide)s in the wavenumber range: 4000–480 cm^{-1} (a); 3500–3200 cm^{-1} (b); 1750–1500 cm^{-1} (c).

vibration appeared at 1658 and 1554 cm^{-1}, respectively (Figure 2c). These results indicate that PHF-*co*-PPAF poly(ester amide)s were successfully prepared.

3.2. Optical properties

Optical properties are an extremely important parameter for various industrial sectors such as, among others, the packaging industry. Therefore, to investigate the optical properties of the PHF-*co*-PPAF poly(ester amide)s, thin films were prepared and characterised by UV-Vis spectroscopy. The UV-Vis transmission spectra of poly(ester amide)s are shown in Figure 3. Neat PHF film showed relatively low transparency, not exceeding 50%. However, as can be clearly observed, along with the increase in PPAF content, the light transmittance also increased. For the PHF-*co*-PPAF 1/0.06 co-polymer, the transparency was very close to 70%. All other PEAs were characterised by high transmittance of visible light, ranging between 85 and 90%, and were optically transparent, as can be seen in the inserted photos in Figure 3. Moreover, all PEAs had a slightly yellow colour. The differences in light transmittance are probably due to the different degrees of crystallinity of the materials. As is known, amorphous materials generally transmit light well, while in the case of semi-crystalline
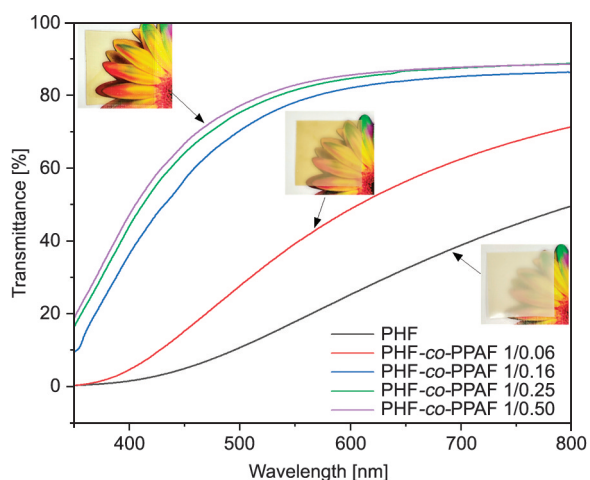

Figure 3. UV-Vis transmittance spectra of PHF and PHF-*co*-PPAF poly(ester amide)s.

materials, light is scattered at the boundaries between the crystalline and amorphous regions.

3.3. Thermal properties

The effects of PPAF units' content on the crystallisation and thermal properties were investigated by DSC with different heating/cooling rates (Figure 4). The obtained thermal results are listed in Table 2. As it can be seen, the glass transition temperature (T_g) increased with the increasing content of PPAF units. This is due to the fact that the hydrogen bonds of

amide groups have a strong rigidifying effect. It is also worth noting here that two of the four synthesised PEAs, containing 0.25 and 0.50 mol% of PPAF co-units exhibited glass transition temperatures higher than room temperature and were completely amorphous. As presented in their work by Cureton *et al.* [33], poly(propylene-furanamide) is an amorphous material, as opposed to PHF homopolymer (Table 2). Thus, for co-polymers with a lower content of PPAF units, the melting and cold crystallisation points are visible on the heating curves. The melting temperatures decrease as the proportion of PPAF units increases. This phenomenon can be explained by thermodynamic interactions between PHF and PPAF,
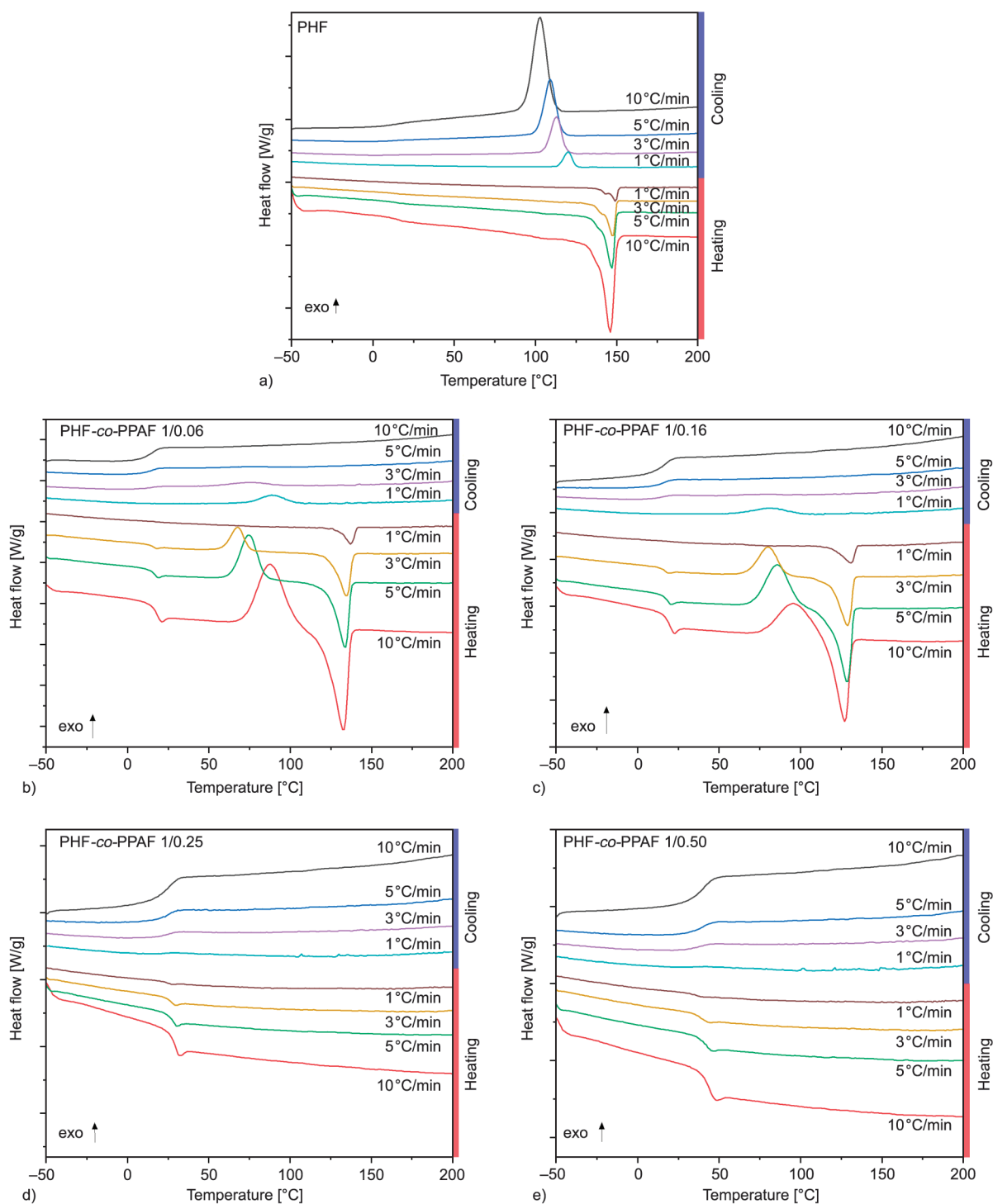

Figure 4. DSC heating and cooling scans at the rates of 10, 5, 3 and 1 °C/min for PHF (a) and PHF-*co*-PPAF poly(ester amide)s compositions (b–e).

such as endothermic interactions between the crystalline part of PHF units and that of the amorphous PPAF units [6]. Moreover, by increasing the proportion of amorphous PPAF units, the thickness of the crystals may be reduced, and they become less stable [50]. The effect of PPAF on the melting behaviour of co-polymers will be investigated in a future paper. In the case of PHF-*co*-PPAF 1/0.06 and PHF-*co*-PPAF 1/0.16 co-polymers, we can also observe cold crystallisation peaks, which, as the heating rate decreases, are shifted to lower temperatures. Importantly, at the lowest heating rate of 1 °C/min, the cold crystallisation exotherms for these co-polymers are almost invisible. At the same time, the melting enthalpies remain almost unchanged. These results indicate that PHF-*co*-PPAF with lower PPAF units' content exhibit slow crystallisation. As shown in Table 2, the degree of crystallinity for PHF-*co*-PPAF 1/0.06 increases from 1.6 to 22.9%, while for PHF-*co*-PPAF 1/0.16 it increases from 0.7 to 25.9%.

An obvious change was observed in the cooling curves of the PEAs compared to neat PHF. As shown in Figure 4a, PHF is semi-crystalline polyester, which crystallises during cooling at about 103 °C. However, PPAF units have a limited crystallisation ability, and the crystallisation temperatures during cooling for selected PEAs are only visible at the slowest heating rates. Moreover, PHF crystallises much faster than the obtained poly(ester amide)s, and its degree of crystallinity, regardless of the heating/cooling rate, is about 25%.

3.4. Thermo-oxidative stability
An important factor in the characteristics of co-polymers is their thermal stability, especially thermo-oxidative stability, which determines the suitability of materials for thermal processing. Thermo-oxidative stability of the synthesised PEAs was measured by TGA, as shown in Figure 5. The characteristic temperatures for mass losses of 5, 10, and 50, as well as the temperatures corresponding to the maximum of mass losses, were listed in Table 3. The thermal degradation of PHF homopolymer and PHF-*co*-PPAF co-polymers occurs in two steps. The PEAs start to

Table 2. Thermal properties of PHF-*co*-PPAF co-polymers.

Sample	Heating rate [°C/min]	T_g [°C]	ΔC_p [J/(g·°C)]	T_{cc} [°C]	ΔH_{cc} [J/g]	T_c [°C]	ΔH_c [J/g]	T_m [°C]	ΔH_m [J/g]	X_c [%]
PHF	10	15	0.12	–	–	103	41.94	146	36.30	25.4
	5	14	0.15	–	–	109	41.82	147	36.44	25.5
	3	15	0.13	–	–	113	40.71	147	36.19	25.3
	1	7	0.17	–	–	120	40.72	149	36.14	25.3
PHF-*co*-PPAF 1/0.06	10	17	0.41	87	32.53	–	–	133	34.84	1.6
	5	16	0.31	74	33.03	–	–	134	35.30	1.6
	3	14	0.22	67	22.57	76	7.592	135	38.02	10.8
	1	18	0.12	–	–	90	38.85	137	32.68	22.9
PHF-*co*-PPAF 1/0.16	10	19	0.33	96	18.13	–	–	127	19.2	0.7
	5	17	0.30	85	36.96	–	–	129	38.24	0.9
	3	16	0.33	80	33.53	–	–	129	38.09	3.2
	1	16	0.05	60	1.44	82	34.82	131	38.57	25.9
PHF-*co*-PPAF 1/0.25	10	28	0.32	–	–	–	–	–	–	0
	5	27	0.32	–	–	–	–	–	–	0
	3	26	0.31	–	–	–	–	–	–	0
	1	24	0.23	–	–	–	–	–	–	0
PHF-*co*-PPAF 1/0.50	10	43	0.30	–	–	–	–	–	–	0
	5	41	0.30	–	–	–	–	–	–	0
	3	39	0.28	–	–	–	–	–	–	0
	1	35	0.38	–	–	–	–	–	–	0

T_g – glass transition temperature;
ΔC_p – specific heat capacity;
T_{cc} – cold crystallisation temperature;
ΔH_{cc} – cold crystallisation enthalpy;
T_m – melting temperature;
ΔH_m – melting enthalpy;
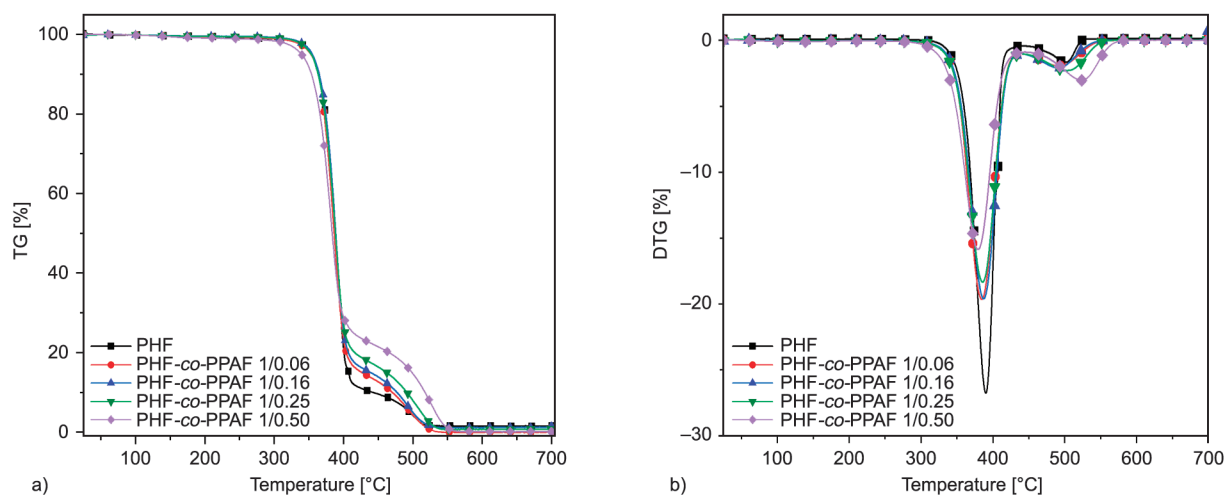X_c – degree of crystallinity.

Figure 5. TG (a) and DTG (b) curves of the PHF and PHF-*co*-PPAF co-polymers under a thermo-oxidative atmosphere.

Table 3. TGA data: temperatures of 5, 10 and 50% mass loss, the temperatures corresponding to the maximum of mass losses (T_{DTG1} and T_{DTG2}) in an oxidising atmosphere.

Sample	$T_{5\%}$ [°C]	$T_{10\%}$ [°C]	$T_{50\%}$ [°C]	T_{DTG1} [°C]	T_{DTG2} [°C]
PHF	354	365	388	390	500
PHF-*co*-PPAF 1/0.06	349	363	386	384	491
PHF-*co*-PPAF 1/0.16	352	364	388	387	490
PHF-*co*-PPAF 1/0.25	350	362	388	385	503
PHF-*co*-PPAF 1/0.50	334	352	383	379	523

degrade at around 320 °C, indicating good thermal stability. The major stage of mass loss is attributed to the main aliphatic chain breakdown and it occurs between 330 and 420 °C. The degradation starting temperature was slightly lower for PEAs, especially with the highest PPAF units content, than for PHF homopolymer. Differences in the initial degradation temperature may result from a greater dispersion of molecular weights and thus from a greater amount of low-molecular products with an increase in the proportion of PPAF units. However, the differences were slight, and there is no significant discrepancy in the temperatures of 50% mass loss between obtained PEAs. Moreover, the temperature of the maximum mass loss in the second degradation step, attributed to the decomposition of the aromatic moieties, increased with an increase in the PPAF units content. All synthesised PEAs had good thermal stability and they are resistant to degradation at processing temperatures up to 300 °C.

3.5. PALS measurements

Measurements of the positron lifetime were carried out to investigate the change of free volume according to the composition of PEAs. The free volume radius and the fraction of the free volume are closely related to the ability to reorganise molecularly and thus are associated with, among others, viscoelasticity, glass transition, and barrier properties of polymers. The results from the PALS analysis were obtained using a three-components fit. Two shorter lifetimes (τ_1, τ_2), insensitive to the structural changes, are attributed to *p–Ps* annihilation and free or trapped positrons, respectively, are not as important as the longest lifetime (τ_3). Thus, Figure 6a illustrates the longest-lived component lifetime (τ_3), which is attributed to the annihilation of *o–Ps*, and the corresponding intensity (I_3) for neat PHF and PHF-*co*-PPAF poly(ester amide)s. As it can be seen, the smallest value of τ_3 of approximately 1.65 ns was obtained for PHF-*co*-PPAF 1/0.50 co-polymer, and the largest one was 1.72 ns for neat PHF. The values of the intensity of this component ranged from 18.8 to 20.4%. As it is known, the value of τ_3 is strictly dependent on the radius of the free volume, according to the Tao-Eldrup relationship, see Figure 4 in Ref. [51], while its intensity depends on the free volume fraction according to Equation (3):

$$f_v = aV_vI_3 \tag{3}$$

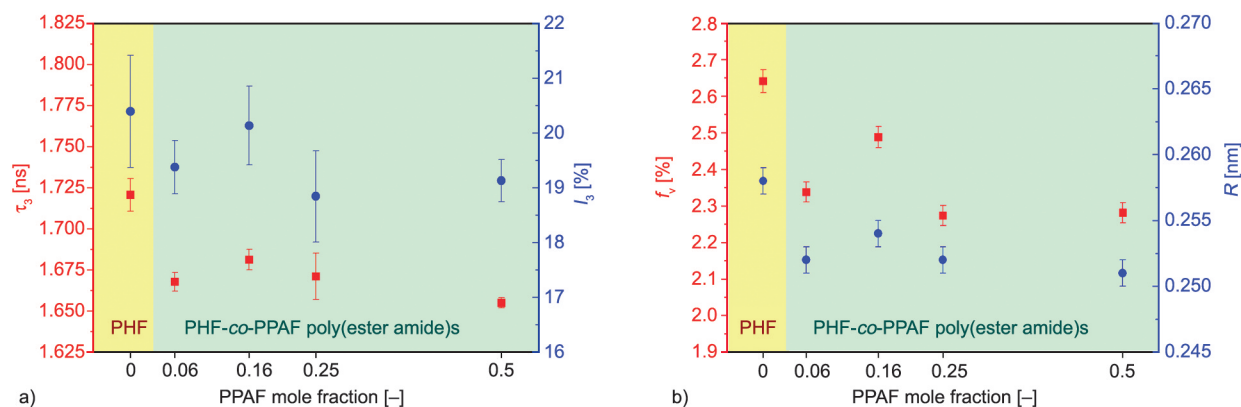where $V_v = 4\pi R^3/3$ is expressed in Å^3 and the coefficient $a = 0.0018$ [51].

Figure 6. The *o–Ps* lifetime (τ_3) (red squares – ■), its intensity (I_3) (blue circles – ●) (a), free volume fraction (f_v) (red squares – ■) and free volume radius (R) (blue circles – ●) (b) for PHF homopolymer and PHF-*co*-PPAF poly(ester amide)s.

Therefore, the calculated values of the free volume radius (R) and the free volume fractions (f_v) are presented in Figure 6b. One can notice a decrease in the free volume radius and their fractions with an increase in the PPAF units' content. In pure PHF, the average f_v was equal to 2.64%. After increasing the content of PPAF units, lower f_v were obtained, ranging from 2.27 to 2.49%, and smaller R values, ranging from 0.251 to 0.255 nm. Generally, the higher the degree of crystallinity of co-polymers, the smaller the free volume radius, which is due to the hindrance of the conformational motion of the macromolecules [52]. However, in the case of synthesised PHF-*co*-PPAF co-polymers, the opposite relationship occurs. It may be related to the glass transition temperature of the obtained materials. The PALS measurements were performed at room temperature, so the co-polymers with the highest content of PPAF units were tested below their T_g, while neat PHF, as well as the co-polymers with the lowest proportion of PPAF, were tested above their T_g. According to the literature, there is a significant relationship between the measurement temperatures, glass transition temperatures, and the τ_3 values [53, 54]. This relationship was discussed in more detail in our previous publication [55].

3.6. Tensile properties

The representative stress-strain curves of PHF homopolymer and synthesised PEAs are shown in Figure 7 and the mechanical properties are listed in Table 4. The mechanical properties of PHF were quite similar to those found in the literature [56, 57]. In the initial deformation stage, the PHF extended until the maximum stress at the yield point was reached, and then a

drop in stress and subsequent strain hardening effect was observed. During stretching, the orientation of the macromolecular chains and crystallisation took place. Synthesised PEAs were characterised by a higher Young's modulus and tensile strength at yield than PHF homopolymer. It is related to the strong intermolecular hydrogen bonds of amide groups, which contribute to the greater PEAs stiffness. On the other hand, elongation at break decreased from 318 % obtained for neat PHF to 75% for PHF-*co*-PPAF 1/0.50 co-polymer. Noticeably, the PEAs with PPAF mole fractions of 6 and 16% achieved lower elongation at break values than the PHF-*co*-PPAF 1/0.25 co-polymer, which is probably related to their higher degree of crystallinity. Among synthesised co-polymers, PHF-*co*-PPAF 1/0.50 was the least flexible material, with elongation at a break of about 75%. Moreover, in the case of this co-polymer, no strain hardening effect occurred. Based on the mechanical and thermal
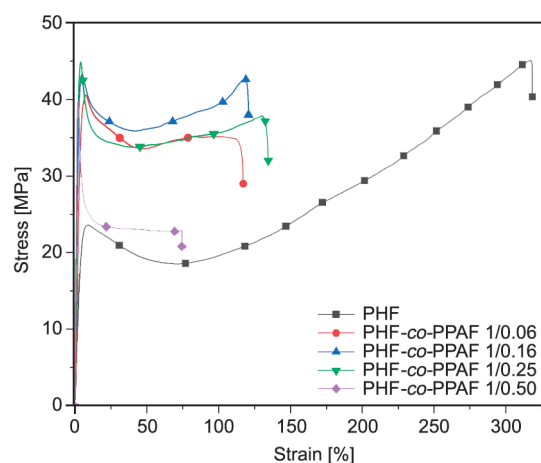

Figure 7. Representative tensile stress-strain curves for PHF homopolymer and PHF-*co*-PPAF poly(ester amide)s.

Table 4. Mechanical properties of synthesised PHF and PHF-*co*-PPAF poly(ester amide)s.

Material	E [MPa]	σ_y [MPa]	ε_y [%]	σ_b [MPa]	ε_b [%]
PHF	394.5±49.8	23.6±0.9	8.8±1.0	45.3±2.9	319.2±13.3
PHF-*co*-PPAF 1/0.06	813.1±99.2	42.4±1.8	6.1±0.9	39.1±4.1	146.3±14.9
PHF-*co*-PPAF 1/0.16	1665.9±165.9	43.3±2.6	5.0±0.4	38.8±3.6	106.6±13.7
PHF-*co*-PPAF 1/0.25	1323.9±204.1	43.7±1.0	2.1±0.2	39.4±2.8	147.1±24.6
PHF-*co*-PPAF 1/0.50	1077.1±182.3	38.4±2.2	2.5±0.7	25.8±3.1	75.3±10.3

E – Young's modulus;
σ_y – tensile strength at yield;
ε_y – elongation at yield;
σ_b – tensile strength at break;
ε_b – elongation at break.

properties of obtained PEAs, it can be seen that the strength and stiffness of co-polymers are significantly influenced by the content of PPAF units, but also by the ability of the co-polymers to crystallise.

4. Conclusions

A series of furan-based poly(ester amide)s were successfully synthesised by the two-stage melt polycondensation method. The compositions and chemical structure were confirmed by ^{1}H NMR and FTIR spectroscopies. Compared to neat PHF, PHF-*co*-PPAF co-polymers were more transparent. With the increase in PPAF units' content, PEAs changed from semi-crystalline to amorphous. Moreover, due to the strong hydrogen bonds of amide groups, glass transition temperature increased with the mole fraction of PPAF units. Furthermore, the thermo-oxidative stability of PEAs was investigated. All obtained materials were thermally stable up to over 300 °C. The results from PALS measurements revealed that with an increase in the content of PPAF units, the free volume fraction and the free volume radius decreased. Moreover, the mechanical properties were investigated. PEAs were characterised by higher Young's modulus and lower elongation at break compared to neat PHF. Both PHF and PHF-*co*-PPAF co-polymers exhibited a strain hardening effect. The mechanical properties of PEAs depended strongly on the PPAF units' content and the crystallinity of PHF units. The above results clearly demonstrate the potential of furan-based poly(ester amide)s, whose properties can be easily controlled depending on the combination of the PHF and PPAF units.

References

[1] Burgess S. K., Leisen J. E., Kraftschik B. E., Mubarak C. R., Kriegel R. M., Koros W. J.: Chain mobility, thermal, and mechanical properties of poly(ethylene furanoate) compared to poly(ethylene terephthalate). Macromolecules, **47**, 1383–1391 (2014).
https://doi.org/10.1021/ma5000199

[2] Terzopoulou Z., Papadopoulos L., Zamboulis A., Papageorgiou D. G., Papageorgiou G. Z., Bikiaris D. N.: Tuning the properties of furandicarboxylic acid-based polyesters with copolymerization: A review. Polymers, **12**, 1209 (2020).
https://doi.org/10.3390/polym12061209

[3] Vannini M., Marchese P., Celli A., Lorenzetti C.: Fully biobased poly(propylene 2,5-furandicarboxylate) for packaging applications: Excellent barrier properties as a function of crystallinity. Green Chemistry, **17**, 4162–4166 (2015).
https://doi.org/10.1039/C5GC00991J

[4] Papageorgiou G. Z., Papageorgiou D. G., Terzopoulou Z., Bikiaris D. N.: Production of bio-based 2,5-furan dicarboxylate polyesters: Recent progress and critical aspects in their synthesis and thermal properties. European Polymer Journal, **83**, 202–229 (2016).
https://doi.org/10.1016/j.eurpolymj.2016.08.004

[5] Burgess S. K., Mikkilineni D. S., Yu D. B., Kim D. J., Mubarak C. R., Kriegel R. M., Koros W. J.: Water sorption in poly(ethylene furanoate) compared to poly(ethylene terephthalate). Part 2: Kinetic sorption. Polymer, **55**, 6870–6882 (2014).
https://doi.org/10.1016/j.polymer.2014.10.065

[6] Burgess S. K., Karvan O., Johnson J. R., Kriegel R. M., Koros W. J.: Oxygen sorption and transport in amorphous poly(ethylene furanoate). Polymer, **55**, 4748–4756 (2014).
https://doi.org/10.1016/j.polymer.2014.07.041

[7] Lotti N., Munari A., Gigli M., Gazzano M., Tsanaktsis V., Bikiaris D. N., Papageorgiou G. Z.: Thermal and structural response of *in situ* prepared biobased poly(ethylene 2,5-furan dicarboxylate) nanocomposites. Polymer, **103**, 288–298 (2016).
https://doi.org/10.1016/j.polymer.2016.09.050

[8] Poulopoulou N., Pipertzis A., Kasmi N., Bikiaris D. N., Papageorgiou D. G., Floudas G., Papageorgiou G. Z.: Green polymeric materials: On the dynamic homogeneity and miscibility of furan-based polyester blends. Polymer, **174**, 187–199 (2019). https://doi.org/10.1016/j.polymer.2019.04.058

[9] Righetti M. C., Marchese P., Vannini M., Celli A., Tricoli F., Lorenzetti C.: Temperature-induced polymorphism in bio-based poly(propylene 2,5-furandicarboxylate). Thermochimica Acta, **677**, 186–193 (2019). https://doi.org/10.1016/j.tca.2018.12.003

[10] Guidotti G., Soccio M., Lotti N., Gazzano M., Siracusa V., Munari A.: Poly(propylene 2,5-thiophenedicarboxylate) *vs.* poly(propylene 2,5-furandicarboxylate): Two examples of high gas barrier bio-based polyesters. Polymers, **10**, 785 (2018). https://doi.org/10.3390/polym10070785

[11] Vannini M., Marchese P., Celli A., Lorenzetti C.: Fully biobased poly(propylene 2,5-furandicarboxylate) for packaging applications: Excellent barrier properties as a function of crystallinity. Green Chemistry, **17**, 4162–4166 (2015). https://doi.org/10.1039/C5GC00991J

[12] Paszkiewicz S., Janowska I., Pawlikowska D., Szymczyk A., Irska I., Lisiecki S., Stanik R., Gude M., Piesowicz E.: New functional nanocomposites based on poly(trimethylene 2,5-furanoate) and few layer graphene prepared by *in situ* polymerization. Express Polymer Letters, **12**, 530–542 (2018). https://doi.org/10.3144/expresspolymlett.2018.44

[13] Zubkiewicz A., Szymczyk A., Sablong R. J., Soccio M., Guidotti G., Siracusa V., Lotti N.: Bio-based aliphatic/aromatic poly(trimethylene furanoate/sebacate) random copolymers: Correlation between mechanical, gas barrier performances and compostability and copolymer composition. Polymer Degradation and Stability, **195**, 109800 (2022). https://doi.org/10.1016/j.polymdegradstab.2021.109800

[14] Soccio M., Martínez-Tong D. E., Alegría A., Munari A., Lotti N.: Molecular dynamics of fully biobased poly (butylene 2,5-furanoate) as revealed by broadband dielectric spectroscopy. Polymer, **128**, 24–30 (2017). https://doi.org/10.1016/j.polymer.2017.09.007

[15] Matos M., Sousa A. F., Mendonça P. V., Silvestre A. J. D.: *Co*-polymers based on poly(1,4-butylene 2,5-furandicarboxylate) and poly(propylene oxide) with tuneable thermal properties: Synthesis and characterization. Materials, **12**, 328 (2019). https://doi.org/10.3390/ma12020328

[16] Kwiatkowska M., Kowalczyk I., Kwiatkowski K., Szymczyk A., Jędrzejewski R.: Synthesis and structure – property relationship of biobased poly(butylene 2,5-furanoate) – block – (dimerized fatty acid) copolymers. Polymer, **130**, 26–38 (2017). https://doi.org/10.1016/j.polymer.2017.10.009

[17] Hu H., Zhang R., Sousa A., Long Y., Ying W. B., Wang J., Zhu J.: Bio-based poly(butylene 2,5-furandicarboxylate)-*b*-poly(ethylene glycol) copolymers with adjustable degradation rate and mechanical properties: Synthesis and characterization. European Polymer Journal, **106**, 42–52 (2018). https://doi.org/10.1016/j.eurpolymj.2018.07.007

[18] Zheng M. Y., Zang X. L., Wang G. X., Wang P. L., Lu B., Ji J. H.: Poly(butylene 2,5-furandicarboxylate-ε-caprolactone): A new bio-based elastomer with high strength and biodegradability. Express Polymer Letters, **11**, 611–621 (2017). https://doi.org/10.3144/expresspolymlett.2017.59

[19] Paszkiewicz S., Irska I., Zubkiewicz A., Szymczyk A., Piesowicz E., Rozwadowski Z., Goracy K.: Biobased thermoplastic elastomers: Structure-property relationship of poly(hexamethylene 2,5-furanodicarboxylate)-block-poly(tetrahydrofuran) copolymers prepared by melt polycondensation. Polymers, **13**, 397 (2021). https://doi.org/10.3390/polym13030397

[20] Kasmi N., Ainali N. M., Agapiou E., Papadopoulos L., Papageorgiou G. Z., Bikiaris D. N.: Novel high Tg fully biobased poly(hexamethylene-*co*-isosorbide-2,5-furan dicarboxylate) copolyesters: Synergistic effect of isosorbide insertion on thermal performance enhancement. Polymer Degradation and Stability, **169**, 108983 (2019). https://doi.org/10.1016/j.polymdegradstab.2019.108983

[21] Papageorgiou G. Z., Tsanaktsis V., Papageorgiou D. G., Chrissafis K., Exarhopoulos S., Bikiaris D. N.: Furan-based polyesters from renewable resources: Crystallization and thermal degradation behavior of poly(hexamethylene 2,5-furan-dicarboxylate). European Polymer Journal, **67**, 383–396 (2015). https://doi.org/10.1016/j.eurpolymj.2014.08.031

[22] Montané J., Armelin E., Asín L., Rodríguez-Galán A., Puiggalí J.: Comparative degradation data of polyesters and related poly(ester amide)s derived from 1,4-butanediol, sebacic acid, and α-amino acids. Journal of Applied Polymer Science, **85**, 1815–1824 (2002). https://doi.org/10.1002/app.10379

[23] Wang R., Ren T., Bai Y., Wang Y., Chen J., Zhang L., Zhao X.: One-pot synthesis of biodegradable and linear poly(ester amide)s based on renewable resources. Journal of Applied Polymer Science, **133**, 43446 (2016). https://doi.org/10.1002/app.43446

[24] Han S., Wu J.: Recent advances of poly(ester amide)s-based biomaterials. Biomacromolecules, **23**, 1892–1919 (2022). https://doi.org/10.1021/acs.biomac.2c00150

[25] Yang Z-Y., Chou Y-L., Yang H-C., Chen C-W., Rwei S-P.: Synthesis and characterization of thermoplastic poly(ester amide)s elastomer (TPEaE) obtained from recycled PET. Journal of Renewable Materials, **9**, 867–880 (2021). https://doi.org/10.32604/jrm.2021.014476

[26] Lips P. A. M., Broos R., van Heeringen M. J. M., Dijkstra P. J., Feijen J.: Synthesis and characterization of poly (ester amide)s containing crystallizable amide segments. Polymer, **46**, 7823–7833 (2005).
https://doi.org/10.1016/j.polymer.2005.07.013

[27] Cao M., Zhang C., He B., Huang M., Jiang S.: Synthesis of 2,5-furandicarboxylic acid-based heat-resistant polyamides under existing industrialization process. Macromolecular Research, **25**, 722–729 (2017).
https://doi.org/10.1007/s13233-017-5070-4

[28] Zubkiewicz A., Paszkiewicz S., Szymczyk A.: Możliwości syntezy poliamidów i kopoliamidów na bazie kwasu 2,5-furanodikarboksylowego oraz jego pochodnych (in Polish). in 'Technologie XXI wieku – aktualne problemy i nowe wyzwania' (eds.: Mołdoch-Mendoń I., Maciąg K.) Wydawnictwo Naukowe TYGIEL, Lublin' Vol. 1, 239–248 (2020).

[29] Mitiakoudis A., Gandini A.: Synthesis and characterization of furanic polyamides. Macromolecules, **24**, 830–835 (1991).
https://doi.org/10.1021/ma00004a003

[30] Ali D. K., Al-Zuheiri A. M., Sweileh B. A.: Green ion-exchange bisfuranic polyamides by polycondensation with bio-based diamines. Green Materials, **8**, 24–31 (2020).
https://doi.org/10.1680/jgrma.18.00091

[31] Fehrenbacher U., Grosshardt O., Kowollik K., Tübke B., Dingenouts N., Wilhelm M.: Synthese und Charakterisierung von Polyestern und Polyamiden auf der Basis von Furan-2,5-dicarbonsäure (in German). Chemie Ingenieur Technik, **81**, 1829–1835 (2009).
https://doi.org/10.1002/cite.200900090

[32] Abid S., El Gharbi R., Gandini A.: Polyamides incorporating furan moieties. 5. Synthesis and characterisation of furan-aromatic homologues. Polymer, **45**, 5793–5801 (2004).
https://doi.org/10.1016/j.polymer.2004.06.046

[33] Cureton L. S. T., Napadensky E., Annunziato C., la Scala J. J.: The effect of furan molecular units on the glass transition and thermal degradation temperatures of polyamides. Journal of Applied Polymer Science, **134**, 45514 (2017).
https://doi.org/10.1002/app.45514

[34] Miyagawa N., Suzuki T., Okano K., Matsumoto T., Nishino T., Mori A.: Synthesis of furan dimer-based polyamides with a high melting point. Journal of Polymer Science Part A: Polymer Chemistry, **56**, 1516–1519 (2018).
https://doi.org/10.1002/pola.29031

[35] Luo K., Wang Y., Yu J., Zhu J., Hu Z.: Semi-bio-based aromatic polyamides from 2,5-furandicarboxylic acid: Toward high-performance polymers from renewable resources. RSC Advances, **6**, 87013–87020 (2016).
https://doi.org/10.1039/c6ra15797a

[36] da Fontoura C. M., Pistor V., Mauler R. S.: Evaluation of degradation of furanic polyamides synthesized with different solvents. Polimeros, **29**, e20190019 (2019).
https://doi.org/10.1590/0104-1428.08917

[37] Moore J. A., Bunting W. W.: Polyesters and polyamides containing isomeric furan dicarboxylic acids. Polymer Science and Technology, **31**, 51–91 (1985).
https://doi.org/10.1007/978-1-4613-2121-7_3

[38] Endah Y. K., Han S. H., Kim J-H., Kim N. K., Kim W. N., Lee H-S., Lee H.: Solid-state polymerization and characterization of a copolyamide based on adipic acid, 1,4-butanediamine, and 2,5-furandicarboxylic acid. Journal of Applied Polymer Science, **133**, 43391 (2016).
https://doi.org/10.1002/app.43391

[39] Jiang Y., Maniar D., Woortman A. J. J., van Ekenstein G. O. R. A., Loos K.: Enzymatic polymerization of furan-2,5-dicarboxylic acid-based furanic-aliphatic polyamides as sustainable alternatives to polyphthalamides. Biomacromolecules, **16**, 3674–3685 (2015).
https://doi.org/10.1021/acs.biomac.5b01172

[40] Jiang Y., Maniar D., Woortman A. J. J., Loos K.: Enzymatic synthesis of 2,5-furandicarboxylic acid-based semi-aromatic polyamides: Enzymatic polymerization kinetics, effect of diamine chain length and thermal properties. RSC Advances, **6**, 67941–67953 (2016).
https://doi.org/10.1039/C6RA14585J

[41] Maniar D., Silvianti F., Ospina V. M., Woortman A. J. J., van Dijken J., Loos K.: On the way to greener furanic-aliphatic poly(ester amide)s: Enzymatic polymerization in ionic liquid. Polymer, **205**, 122662 (2020).
https://doi.org/10.1016/j.polymer.2020.122662

[42] Cousin T., Galy J., Rousseau A., Dupuy J.: Synthesis and properties of polyamides from 2,5-furandicarboxylic acid. Journal of Applied Polymer Science, **135**, 45901 (2018).
https://doi.org/10.1002/app.45901

[43] Wilsens C. H. R. M., Deshmukh Y. S., Noordover B. A. J., Rastogi S.: Influence of the 2,5-furandicarboxamide moiety on hydrogen bonding in aliphatic–aromatic poly (ester amide)s. Macromolecules, **47**, 6196–6206 (2014).
https://doi.org/10.1021/ma501310f

[44] Papadopoulos L., Klonos P. A., Kluge M., Zamboulis A., Terzopoulou Z., Kourtidou D., Magaziotis A., Chrissafis K., Kyritsis A., Bikiaris D. N., Robert T.: Unlocking the potential of furan-based poly(ester amide)s: An investigation of crystallization, molecular dynamics and degradation kinetics of novel poly(ester amide)s based on renewable poly(propylene furanoate). Polymer Chemistry, **12**, 5518–5534 (2021).
https://doi.org/10.1039/D1PY00713K

[45] Zubkiewicz A., Irska I., Miadlicki P., Walkowiak K., Rozwadowski Z., Paszkiewicz S.: Structure, thermal and mechanical properties of copoly(ester amide)s based on 2,5-furandicarboxylic acid. Journal of Materials Science, **56**, 19296–19309 (2021).
https://doi.org/10.1007/s10853-021-06576-9

[46] Jiang M., Liu Q., Zhang Q., Ye C., Zhou G.: A series of furan-aromatic polyesters synthesized via direct esterification method based on renewable resources. Journal of Polymer Science Part A: Polymer Chemistry, **50**, 1026–1036 (2012).
https://doi.org/10.1002/pola.25859

[47] Sanusi O. M., Papadopoulos L., Klonos P. A., Terzopoulou Z., Hocine N. A., Benelfellah A., Papageorgiou G. Z., Kyritsis A., Bikiaris D. N.: Calorimetric and dielectric study of renewable poly(hexylene 2,5-furan-dicarboxylate)-based nanocomposites *in situ* filled with small amounts of graphene platelets and silica nanoparticles. Polymers, **12**, 1239 (2020).
https://doi.org/10.3390/polym12061239

[48] Gharbi S., Gandini A.: Polyamides incorporating furan moieties. 1. Interfacial polycondensation of 2,2′-bis(5-chloroformyl-2-furyl)propane with 1,6-diaminohexane. Acta Polymerica, **7**, 293–297 (1999).
https://doi.org/10.1002/(SICI)1521-4044(19990801)50:8<293::AID-APOL293>3.0.CO;2-I

[49] Ge Y. P., Yuan D., Luo Z. L., Wang B. B.: Synthesis and characterization of poly(ester amide) from renewable resources through melt polycondensation. Express Polymer Letters, **8**, 50–54 (2014).
https://doi.org/10.3144/expresspolymlett.2014.6

[50] Hoffman J. D., Weeks J. J.: Melting process and the equilibrium melting temperature of polychlorotrifluoroethylene. Journal of Research of the National Bureau of Standards Section A: Physics and Chemistry, **66**, 13–28 (1962).
https://doi.org/10.6028/jres.066A.003

[51] Wang Y. Y., Nakanishi H., Jean Y. C., Sandreczki T. C.: Positron annihilation in amine-cured epoxy polymers–pressure dependence. Journal of Polymer Science Part B: Polymer Physics, **28**, 1431–1441 (1990).
https://doi.org/10.1002/polb.1990.090280902

[52] Bryaskova R., Mateva R., Djourelov N., Krasteva M.: Study of multiblock polyamide-6/Poly-(isoprene) copolymers by positron annihilation spectroscopy. Open Chemistry, **6**, 575–580 (2008).
https://doi.org/10.2478/s11532-008-0073-9

[53] Bartoš J., Šauša O., Schwartz G. A., Alegría A., Alberdi J. M., Arbe A., Krištiak J., Colmenero J.: Positron annihilation and relaxation dynamics from dielectric spectroscopy and nuclear magnetic resonance: Cis–trans-1,4-poly(butadiene). The Journal of Chemical Physics, **134**, 164507 (2011).
https://doi.org/10.1063/1.3578446

[54] Bartoš J., Schwartz G. A., Šauša O., Alegría A., Krištiak J., Colmenero J.: Positron annihilation response and broadband dielectric spectroscopy: *Poly(propylene glycol)*. Journal of Non-Crystalline Solids, **356**, 782–786 (2010).
https://doi.org/10.1016/j.jnoncrysol.2009.09.043

[55] Irska I., Paszkiewicz S., Pawlikowska D., Dryzek J., Linares A., Nogales A., Ezquerra T. A., Piesowicz E.: Relaxation behaviour and free volume of bio-based poly(trimethylene terephthalate)-block-poly(caprolactone) copolymers as revealed by broadband dielectric and positron annihilation lifetime spectroscopies. Polymer, **229**, 123949 (2021).
https://doi.org/10.1016/j.polymer.2021.123949

[56] Jiang M., Liu Q., Zhang Q., Ye C., Zhou G.: A series of furan-aromatic polyesters synthesized *via* direct esterification method based on renewable resources. Journal of Polymer Science Part A: Polymer Chemistry, **50**, 1026–1036 (2012).
https://doi.org/10.1002/pola.25859

[57] Chen M., Jiang Z., Qiu Z.: Synthesis and properties of poly(hexamethylene 2,5-furandicarboxylate-*co*-adipate) copolyesters. European Polymer Journal, **161**, 110860 (2021).
https://doi.org/10.1016/j.eurpolymj.2021.110860